

A Copper(I) Homocubane Collapses to a Tetracapped Tetrahedron Upon Hydride Insertion

Ping-Kuei Liao,[†] Kuan-Guan Liu,[†] Ching-Shiang Fang,[†] C. W. Liu,^{*,†} John P. Fackler, Jr.,^{*,†} and Ying-Yann Wu[‡]

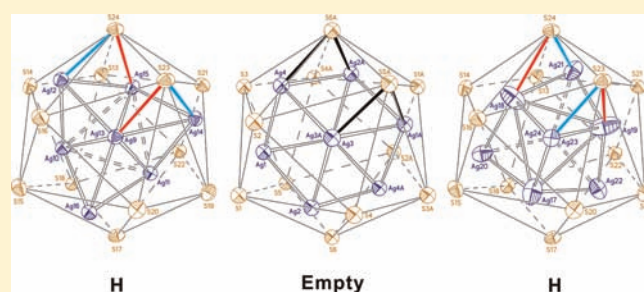
[†]Department of Chemistry, National Dong Hwa University, Hualien, Taiwan 97401, R. O. C.

[‡]Department of Chemistry, Texas A&M University, College Station, TX 77842-3012, United States

[§]Rezwave Techology Inc. His-Chih, Taiwan, R. O. C.

S Supporting Information

ABSTRACT: The hydrido copper(I) and silver(I) clusters incorporating 1,1-dicyanoethylene-2,2-dithiolate (*i*-MNT) ligands are presented in this paper. Reactions of M(I) (M = Cu, Ag) salts, [Bu₄N]₂[S₂CC(CN)₂], with the anion sources ([Bu₄N][BH₄]⁻ for H⁻, [Bu₄N][BD₄]⁻ for D⁻) in an 8:6:1 molar ratio in THF produce octanuclear penta-anionic Cu(I)/Ag(I) clusters, [Bu₄N]₅[M₈(X){S₂CC(CN)₂}₆] (M = Cu, X = H, **1_H**; X = D, **1_D**; M = Ag, X = H, **2_H**; X = D, **2_D**). They can also be produced from the stoichiometric reaction of M₈(*i*-MNT)₆⁴⁻ with the ammonium borohydride. All four compounds have been fully characterized spectroscopically (¹H and ¹³C NMR, IR, UV–vis) and by elemental analyses. The deuteride-encapsulated Cu₈/Ag₈ clusters of **1_D** and **2_D** are also characterized by ²H NMR. X-ray crystal structures of **1_H** and **2_H** reveal a hydride-centered tetracapped tetrahedral Cu₈/Ag₈ core, which is inscribed within an S₁₂ icosahedron formed by six *i*-MNT ligands, each in a tetrametallic–tetraconnective (μ₂, μ₂) bonding mode. The encapsulated hydride in **2_H** is unequivocally characterized by both ¹H and ¹⁰⁹Ag NMR spectroscopies, and the results strongly suggest that the hydride is coupled to eight magnetically equivalent silver nuclei on the NMR time scale. Therefore, a fast interchange between the vertex and capping silver atoms in solution gives a plausible explanation for the perceived structural differences between the Ag₈ geometry deduced from the X-ray structure and the NMR spectra.



INTRODUCTION

The first discrete, octanuclear copper complex [Cu₈{S₂CC(CN)₂}₆]⁴⁻ (S₂CC(CN)₂²⁻ = *i*-MNT) in which eight copper atoms are arranged at the vertices of a cube and each square face of the cube is capped by a 1,1-dithiolato ligand was synthesized by Fackler and Coucouvanis in 1968.¹ Restricted by the face-bridging dithiolato ligands, the 4-fold rotational axes identified in the Cu₈ cube no longer existed in the Cu₈S₁₂ skeleton. Hence, the cluster anion has an idealized T_h symmetry, the first of any copper compounds. It had been believed that only dianionic 1,1- or 1,2-dithiolato ligands can produce the octanuclear T_h molecular cluster.² Nonetheless, recent synthetic advances have expanded the ligand possibilities utilizing various 1,1-dithioacids (uninegative charge), including dithiocarbamates,³ dithiophosph(in)ates,⁴ and their selenium analogs, diselenophosphates,⁵ to yield a family of cluster compounds having the same structural type, but as cluster cations of +2 charge.

The mass spectrum of the homocubane copper cluster anion, [Cu₈{S₂CC(CN)₂}₆]⁴⁻, was determined by ²⁵²Cf-plasma desorption MS.⁶ Two principal peaks were observed in the high mass range at *m/z* 2569 and 2812 in the positive ion ²⁵²Cf-PD mass spectrum of [(Bu₄N)₄Cu₈(*i*-MNT)₆]. The structure of the

m/z 2569 peak corresponds to the intact complex containing an additional *n*-butyl ammonium ion to form the adduct ion, [(*n*-Bu₄N)₅Cu₈(*i*-MNT)₆]⁺ (*M*_{calc} = 2562). The mass of the second peak is 243 mass units higher than that of the adduct ion. This mass difference fits well as the mass of the *n*-Bu₄N⁺ ion (242 u), and it was proposed that the structure of the second peak likely corresponds to the addition of a hydride ion to the tetravalent anion. Thus, the formula of this ion would correspond to [(*n*-Bu₄N)₆Cu₈(H){S₂CC(CN)₂}₆]⁺ (*M*_{calc} = 2805). In addition, symmetry considerations for the Cu₈S₁₂ T_h cluster suggested that the linear combinations of the eight individual accepting orbitals, which point toward the center of the cube, on each of the three coordinate, 16-electron Cu^I centers give this set of a_g + t_u + t_g + a_u orbitals.^{5,7} Thus, it seemed possible that the a_g orbital can be filled with two (hydride) electrons or with eight valence (halide or chalcogenide, a_g and t_u) electrons in the formation of closed-shell anion-centered Cu₈S₁₂ clusters. Hence, the species M₈L₆⁵⁻ was tentatively assigned as an M₈HL₆⁵⁻ with a hydride, H⁻, encapsulated in the center of the Cu₈ cubane in T_h

Received: May 11, 2011

Published: August 01, 2011

symmetry. Nevertheless, a synthetic approach was needed to confirm the existence of a hydride-centered cluster.

The possibility of incorporating one hydride at the center of a copper cubane was not realized until a series of $[\text{Cu}_8(\text{H})\{\text{E}_2\text{P}(\text{OR})_2\}_6]^+$ ($\text{E} = \text{S}, \text{Se}$; $\text{R} = \text{Et}, \text{iPr}$) complexes were structurally authenticated as hydride-centered tetracapped tetrahedral copper skeletons inscribed within an icosahedral chalcogen cage, as reported by the Liu's group in 2009.^{4,5} Structure distortions (or contractions) of the copper framework from a cube to a tetracapped tetrahedron was totally unprecedented in the metal hydrido cluster chemistry. First, hydride-encapsulated metal clusters normally display a metal framework expansion, such as those observed in $[\text{HCo}_6(\text{CO})_{15}]^-$,⁸ a 6-coordinate hydride in the octahedral cavity, verified by a neutron diffraction study. Second, due to the lack of an inversion center for a tetracapped tetrahedron, the idealized T_h symmetry of the parent cubane was reduced to T symmetry in the hydride-centered Cu_8 clusters. Because the hydride is spherical, symmetry breaking had occurred. This is indeed different from the original symmetry considered for a hypothetical hydride-centered molecule, $[(n\text{-Bu}_4\text{N})_6\text{Cu}_8(\text{H})(i\text{-MNT})_6]^+$ with T_h symmetry, the species suggested from the mass spectrometry results.⁶ To test the generality of the framework distortion (or contraction) observed in the Cu_8H cluster core by varying the cluster charge, we decided to study again the dinegative 1,1-dithiolate ligand with the aim that the accommodation of a hydride at the center of the tetravalent anionic cluster might indeed be achieved. Herein, we report the detailed synthesis and X-ray structure of the long sought after anion $[\text{Cu}_8(\text{H})\{\text{S}_2\text{CC}(\text{CN})_2\}_6]^{5-}$. The silver analogue, $[\text{Ag}_8(\text{H})\{\text{S}_2\text{CC}(\text{CN})_2\}_6]^{5-}$, is also characterized, and the encapsulated hydride is unequivocally characterized by both ^1H and ^{109}Ag NMR spectroscopies.

EXPERIMENTAL SECTION

All chemicals were purchased from commercial sources and used as received. Solvents were purified following standard protocols. All the reactions were performed in oven-dried Schlenk glassware and carried out under a N_2 atmosphere by using standard inert atmosphere techniques.⁹ The elemental analyses were done using a PerkinElmer 2400 CHN analyzer. NMR spectra were recorded on a Bruker Advance DPX300 FT-NMR spectrometer that operates at 300 MHz while recording ^1H , 46.1 MHz for ^2H , and 75.5 MHz for ^{13}C NMR. The ^{109}Ag NMR spectra of $\mathbf{2}_\text{H}$ were recorded on a Bruker Advance II 600NMR that operates at 27.9 MHz. The chemical shift (δ) and coupling constant (J) are reported in parts per million and hertz, respectively. Melting points were measured by using a Fargo MP-2D melting point apparatus. All infrared spectra were recorded on a Bruker Optics FTIR TENSOR 27 spectrometer ($180\text{--}4000\text{ cm}^{-1}$) at $20\text{ }^\circ\text{C}$ using CsI plates. UV–visible spectra were measured on a PerkinElmer Lambda 750 spectrophotometer.

Synthesis. $[\text{Bu}_4\text{N}]_5[\text{Cu}_8(\text{H})\{\text{S}_2\text{CC}(\text{CN})_2\}_6]$ ($\mathbf{1}_\text{H}$). *Method (a).* $[\text{Cu}(\text{CH}_3\text{CN})_4](\text{PF}_6)$ (0.239 g, 0.64 mmol) and $[\text{Bu}_4\text{N}]_2[\text{S}_2\text{CC}(\text{CN})_2]$ (0.3 g, 0.48 mmol) were charged in a 100 mL flask, and 40 mL of THF was added to it. The solution was stirred at RT for 1 h to form the orange solution. $(\text{Bu}_4\text{N})(\text{BH}_4)$ (0.021 g, 0.08 mmol) was added to this solution and stirred for 3 h. It was then filtered to get rid of any solids, and the filtrate was evaporated to dryness under vacuum. It was washed with MeOH, and then the solid was dried under vacuum to obtain $[\text{Bu}_4\text{N}]_5[\text{Cu}_8(\text{H})\{\text{S}_2\text{CC}(\text{CN})_2\}_6]$ as a brown powder. Yield: 0.131 g (64%).

Method (b). To a solution of $[\text{Bu}_4\text{N}]_4[\text{Cu}_8\{\text{S}_2\text{CC}(\text{CN})_2\}_6]$ (0.3 g, 0.13 mmol) in 50 mL of THF was added $(\text{Bu}_4\text{N})(\text{BH}_4)$ (0.033 g, 0.13 mmol). The mixture was stirred at room temperature for 3 h. It was then

filtered to get rid of any solids, and the filtrate was evaporated to dryness under vacuum. It was washed with MeOH, and then the solid was dried under vacuum to obtain $[\text{Bu}_4\text{N}]_5[\text{Cu}_8(\text{H})\{\text{S}_2\text{CC}(\text{CN})_2\}_6]$ as a brown powder. Yield: 0.239 g (72%). mp: $217\text{ }^\circ\text{C}$ decomposed. Anal. Calcd for $\text{Cu}_8\text{H}_{181}\text{C}_{104}\text{N}_{17}\text{S}_{12} \cdot 2\text{CH}_3\text{OH}$: C, 48.47; H, 7.25; N, 9.06. Found: C, 48.62; H, 6.93; N, 8.79%. ^1H NMR (300 MHz, acetone- d_6): 1.00 (t, $^3J_{\text{HH}} = 7.4\text{ Hz}$, 60H, CH_3), 1.43 (m, 40H, CH_2), 1.82 (m, 40H, CH_2), 3.38 (t, $^3J_{\text{HH}} = 7.4\text{ Hz}$, 40H, CH_2), 7.66 (bs, 1H, $\mu_4\text{-H}$). ^{13}C NMR (75.5 MHz, acetone- d_6): 13.2, 19.8, 23.8, 59.1, 76, 118.1, 205.5 ppm. IR (CsI, cm^{-1}): $\nu(\text{CN})$, 2197 (s); $\nu(\text{C}=\text{C})$, 1390 (s); $\nu(\text{C}-\text{S})$, 920 (s); $\nu(\text{Cu}-\text{S})$, 247 (m), 220 (m), 200 (m). UV–vis [λ_{max} in nm, (ϵ in $\text{M}^{-1}\text{ cm}^{-1}$): 312 (66 000), 417 (88 000)].

$[\text{Bu}_4\text{N}]_5[\text{Cu}_8(\text{D})\{\text{S}_2\text{CC}(\text{CN})_2\}_6]$ ($\mathbf{1}_\text{D}$). This was synthesized in a similar procedure as that described for $\mathbf{1}_\text{H}$ by using $(\text{Bu}_4\text{N})(\text{BD}_4)$ instead of $(\text{Bu}_4\text{N})(\text{BH}_4)$. Yield: 0.106 g (52%). mp: $213\text{ }^\circ\text{C}$ decomposed. Anal. Calcd for $\text{Cu}_8\text{H}_{180}\text{D}_1\text{C}_{104}\text{N}_{17}\text{S}_{12}$: C, 48.72; H, 7.16; N, 9.29. Found: C, 48.66; H, 6.90; N, 8.90%. ^1H NMR (300 MHz, acetone- d_6): 1.00 (t, $^3J_{\text{HH}} = 7.4\text{ Hz}$, 60H, CH_3), 1.43 (m, 40H, CH_2), 1.82 (m, 40H, CH_2), 3.38 (t, $^3J_{\text{HH}} = 7.4\text{ Hz}$, 40H, CH_2). ^2H NMR (acetone, δ , ppm): 7.60 (bs, 1D). ^{13}C NMR (75.5 MHz, acetone- d_6): 13.2, 19.8, 23.8, 59.1, 76.2, 118.5, 205.3 ppm. IR (CsI, cm^{-1}): $\nu(\text{CN})$, 2196 (s); $\nu(\text{C}=\text{C})$, 1388 (s); $\nu(\text{C}-\text{S})$, 920 (s); $\nu(\text{Cu}-\text{S})$, 247 (m), 221 (m), 201 (m). UV–vis [λ_{max} in nm, (ϵ in $\text{M}^{-1}\text{ cm}^{-1}$): 311 (65 400), 419 (87 200)].

$[\text{Bu}_4\text{N}]_5[\text{Ag}_8(\text{H})\{\text{S}_2\text{CC}(\text{CN})_2\}_6]$ ($\mathbf{2}_\text{H}$). *Method (a).* AgNO_3 (0.108 g, 0.64 mmol) and $[\text{Bu}_4\text{N}]_2[\text{S}_2\text{CC}(\text{CN})_2]$ (0.3 g, 0.48 mmol) were charged in a 100 mL flask, and 40 mL of THF was added to it. The solution was stirred at $-20\text{ }^\circ\text{C}$ for 1 h to form the yellow solution. $(\text{Bu}_4\text{N})(\text{BH}_4)$ (0.021 g, 0.08 mmol) was added to this solution and stirred for 3 h. It was then filtered to get rid of any solids, and the filtrate was evaporated to dryness under vacuum. It was washed with MeOH, and then the solid was dried under vacuum to obtain $[\text{Bu}_4\text{N}]_5[\text{Ag}_8(\text{H})\{\text{S}_2\text{CC}(\text{CN})_2\}_6]$ as a pale-green powder. Yield: 0.111 g (48%).

Method (b). To a solution of $[\text{Bu}_4\text{N}]_4[\text{Ag}_8\{\text{S}_2\text{CC}(\text{CN})_2\}_6]$ (0.3 g, 0.11 mmol) in 50 mL of THF was added $(\text{Bu}_4\text{N})(\text{BH}_4)$ (0.029 g, 0.11 mmol). The mixture was stirred at $-20\text{ }^\circ\text{C}$ for 3 h. It was then filtered to get rid of any solids, and the filtrate was evaporated to dryness under vacuum. It was washed with MeOH, and then the solid was dried under vacuum to obtain $[\text{Bu}_4\text{N}]_5[\text{Ag}_8(\text{H})\{\text{S}_2\text{CC}(\text{CN})_2\}_6]$ as a pale-green powder. Yield: 0.167 g (51%). mp: $173\text{ }^\circ\text{C}$ decomposed. Anal. Calcd for $\text{Ag}_8\text{H}_{181}\text{C}_{104}\text{N}_{17}\text{S}_{12} \cdot 3\text{H}_2\text{O}$: C, 42.04; H, 6.34; N, 8.01. Found: C, 42.05; H, 6.10; N, 7.92%. ^1H NMR (300 MHz, acetone- d_6): 1.00 (t, $^3J_{\text{HH}} = 7.4\text{ Hz}$, 60H, CH_3), 1.43 (m, 40H, CH_2), 1.82 (m, 40H, CH_2), 3.38 (t, $^3J_{\text{HH}} = 7.4\text{ Hz}$, 40H, CH_2), 9.65 (nonet, $J_{\text{HAg}} = 28.86\text{ Hz}$, 1H). ^{13}C NMR (75.5 MHz, acetone- d_6): 13.3, 19.8, 23.8, 59.0, 78.2, 118.1, 207.0 ppm. IR (CsI, cm^{-1}): $\nu(\text{CN})$, 2197 (s); $\nu(\text{C}=\text{C})$, 1383 (s); $\nu(\text{C}-\text{S})$, 919 (s); $\nu(\text{Ag}-\text{S})$, 225 (m), 193 (m). UV–vis [λ_{max} in nm, (ϵ in $\text{M}^{-1}\text{ cm}^{-1}$): 294 (66 000), 367 (186 000)].

$[\text{Bu}_4\text{N}]_5[\text{Ag}_8(\text{D})\{\text{S}_2\text{CC}(\text{CN})_2\}_6]$ ($\mathbf{2}_\text{D}$). This was synthesized in a similar procedure as that described for $\mathbf{2}_\text{H}$ by replacing using $(\text{Bu}_4\text{N})(\text{BD}_4)$ with $(\text{Bu}_4\text{N})(\text{BD}_4)$. Yield: 0.103 g (43%). mp: $166\text{ }^\circ\text{C}$ decomposed. Anal. Calcd for $\text{Ag}_8\text{H}_{180}\text{D}_1\text{C}_{104}\text{N}_{17}\text{S}_{12}$: C, 42.80; H, 6.29; N, 8.16. Found: C, 42.90; H, 6.30; N, 8.30%. ^1H NMR (300 MHz, acetone- d_6): 1.00 (t, $^3J_{\text{HH}} = 7.4\text{ Hz}$, 60H, CH_3), 1.43 (m, 40H, CH_2), 1.82 (m, 40H, CH_2), 3.38 (t, $^3J_{\text{HH}} = 7.4\text{ Hz}$, 40H, CH_2). ^2H NMR (acetone, δ , ppm): 9.64 (bs, 1D). ^{13}C NMR (75.5 MHz, acetone- d_6): 13.3, 19.8, 23.8, 59.0, 78.1, 118.5, 207.1 ppm. IR (CsI, cm^{-1}): $\nu(\text{CN})$, 2198 (s); $\nu(\text{C}=\text{C})$, 1383 (s); $\nu(\text{C}-\text{S})$, 920 (s); $\nu(\text{Ag}-\text{S})$, 224 (m), 194 (m). UV–vis [λ_{max} in nm, (ϵ in $\text{M}^{-1}\text{ cm}^{-1}$): 294 (67 300), 365 (181 000)].

X-ray Crystallography. Single crystals of $\mathbf{1}_\text{H}$ and $\mathbf{2}_\text{H}$ suitable for X-ray diffraction experiments were obtained by diffusing hexane into an acetone solution and a dichloromethane solution of the compounds, respectively. Crystals were mounted on the tips of glass fibers with epoxy resin. Data were collected on a Bruker APEXII CCD diffractometer using graphite monochromated Mo K α radiation ($\lambda = 0.71073\text{ \AA}$).

Table 1. Crystallographic Data for **1_H** and **2_H**

	1_H ·C ₃ H ₆ O	2_H ·1/2C ₄ H ₈ O·1/2CH ₂ Cl ₂
formula	C ₂₁₁ H ₃₆₈ Cu ₁₆ N ₃₄ O ₁ S ₂₄	C _{210.5} H ₃₆₇ Ag ₁₆ Cl ₁ N ₃₄ O _{0.5} S ₂₄
fw	5183.47	5913.19
cryst symmetry	triclinic	triclinic
space group	P1	P1
<i>a</i> , Å	16.9201(18)	17.156(2)
<i>b</i> , Å	16.9808(18)	17.168(2)
<i>c</i> , Å	24.707(3)	24.973(3)
α, deg	76.071(2)	76.090(3)
β, deg	73.921(2)	73.629(3)
γ, deg	76.239(2)	75.597(3)
<i>V</i> , Å ³	6508.0(12)	6719.9(14)
<i>Z</i>	1	1
<i>T</i> , K	253(2)	253(2)
ρ _{calc} , g/cm ³	1.321	1.471
μ, mm ⁻¹	1.521	1.384
reflns collected	76972	59341
independent reflns	46136 (<i>R</i> _{int} = 0.0358)	42635 (<i>R</i> _{int} = 0.0253)
data/restraints/ params	46136/29/2627	42635/33/2559
final <i>R</i> indices [<i>I</i> > 2σ(<i>I</i>) ^{a,b}]	0.0470	0.0555
<i>R</i> indices (all data)	0.1408	0.1581
GOF	1.040	1.021
Δρ _{max} , e Å ⁻³	1.026	2.375
Δρ _{min} , e Å ⁻³	-0.401	-1.536
^a <i>RI</i> = Σ <i>F</i> _o - <i>F</i> _c /Σ <i>F</i> _o . ^b <i>wR2</i> = {Σ[<i>w</i> (<i>F</i> _o ² - <i>F</i> _c ²) ²]/Σ[<i>w</i> (<i>F</i> _o ²)]} ^{1/2} .		

Absorption corrections for the area detector were performed with the program SADABS.¹⁰ Structures were solved by direct methods and were refined against the least-squares methods on *F*² with the SHELXL-97 package,¹¹ incorporated in SHELXTL/PC V5.10.¹² All Cu atoms in **1_H** were disordered in two positions with the major component in 75% occupancy. Eight silver atoms in **2_H** were also disordered in two positions with the major component in 75% occupancy. Several carbon atoms of the tetrabutylammonium cations in both **1_H** and **2_H** were found disordered and thus were refined isotropically. Restraints to the alkyl side chains were applied in some cases, and they were described in the CIF. H atoms on the tetrabutylammonium cations were added at idealized positions except for the disordered carbon atoms of the alkyl side chains. The central hydrides were located from the different Fourier map and refined isotropically. Crystallographic details for compounds **1_H** and **2_H** are given in Table 1.

RESULTS AND DISCUSSION

Synthesis and Spectroscopy. The hydrido copper clusters, [Bu₄N]₅[Cu₈(H)(*i*-MNT)₆], **1_H**, and [Bu₄N]₅[Cu₈(D)(*i*-MNT)₆], **1_D**, are obtained by the reaction of Cu(CH₃CN)₄PF₆ with [Bu₄N]₂[S₂CC(CN)₂] in an 8:6 molar ratio for 1 h in THF, followed by the addition of 1 equiv of (Bu₄N)(BH₄) ((Bu₄N)(BD₄)) at ambient temperature. Presumably, the parent cubane, [Bu₄N]₄[Cu₈(*i*-MNT)₆], was formed first, followed by the hydride insertion, to yield the desired compound, and this indeed was confirmed by the reaction of [Bu₄N]₄[Cu₈(*i*-MNT)₆] with borohydride in solution. The infrared spectrum of **1_H** is very similar to that of the parent Cu₈ cubane, [Bu₄N]₄[Cu₈(*i*-MNT)₆]. The IR spectrum of **1_H** displays an absorption band at 2197 cm⁻¹

(ν(CN)), which is similar to that of the Cu₈ cubic cluster, [Bu₄N]₄[Cu₈(*i*-MNT)₆], at 2207 cm⁻¹. Compound **1_H** also shows three Cu–S stretching bands at 247, 222, and 200 cm⁻¹, whereas the Cu₈ cubic cluster shows similar Cu–S stretching peaks at 247 and 230 cm⁻¹. The UV–vis spectrum of **1_H** shows two absorption bands at about 417 (ε = 88 000 M⁻¹ cm⁻¹) and 312 (ε = 66 000 M⁻¹ cm⁻¹) in DCM. The results are also similar to those of the Cu₈ cube.¹³ Besides the chemical shifts of the carbon atoms of the butyl groups, the ¹³C NMR of **1_H** shows three resonances, 205.5, 118.1, and 76.0 ppm, which are assigned to the chemical shifts of a CS₂ moiety, a cyano group, and an olefinic unit, respectively, and shifted slightly by comparison to the corresponding resonances of the Cu₈ cube (198, 117, and 80 ppm).¹³ The ¹H NMR spectrum of **1_H** displays a set of chemical shifts corresponding to the butyl group. In addition, a broad peak centered at 7.60 ppm that integrates to 1H relative to 40 methylene protons of 5 tetrabutylammonium cations is observed. Peak broadening is due to the coupling to a quadruple nuclei of copper (*I* = 3/2).⁵ Furthermore, **1_D** exhibits a peak at 7.60 ppm in the ²H NMR spectrum, which originated from the entrapped deuteride. A significant downfield shift for the hydride resonance of **1_H** is revealed by comparison with [Cu₈(H){S₂P(OR)₂}₆]⁺,^{4b} and [Cu₈(H){Se₂P(OR)₂}₆]⁺,⁵ whose hydride chemical shifts are at 3.69 and -0.58 ppm, respectively.

To observe the scalar couplings between the hydride and its peripheral metal atoms in the ¹H NMR spectrum where only a broad singlet in **1_H** was detected, the NMR-active nuclei of silver (^{107/109}Ag, *I* = 1/2) afforded this opportunity. The reaction of AgNO₃ and [Bu₄N]₂[S₂CC(CN)₂] in an 8:6 molar ratio in THF at -20 °C for 1 h, followed by the addition of 1 equiv of [Bu₄N][BH₄] ([Bu₄N][BD₄]), produced [Bu₄N]₅[Ag₈(H)(*i*-MNT)₆], **2_H**, and [Bu₄N]₅[Ag₈(D)(*i*-MNT)₆], **2_D**, respectively. The compound **2_H** was structurally characterized. The IR spectrum of **2_H** displays an absorption band at 2197 cm⁻¹ (ν(CN)), which is similar to that of the Ag₈ cubic cluster, [Bu₄N]₄[Ag₈(*i*-MNT)₆], at 2204 cm⁻¹. Instead of the 220 and 205 cm⁻¹ bands (Ag–S stretching) observed for a Ag₈ cubane, the compound **2_H** shows two bands at 225 and 193 cm⁻¹. The UV–vis spectrum of **2_H** shows two absorption bands at 367 (ε = 186 000 M⁻¹ cm⁻¹) and 294 (ε = 66 000 M⁻¹ cm⁻¹) in DCM that are almost identical to those in the Ag₈ cube.

At 293 K, the ¹H NMR spectrum of **2_H** displays chemical shifts corresponding to the butyl group, and an apparent nonet resonance centered at 9.65 ppm that integrates to 1H relative to 60 methyl protons of a total of 5 tetrabutylammonium cations. This peak could correspond to the hydride resonance. Surprisingly, the nonet peak started to split at 273 K and was resolved into a nonet of nonets at 263 K. Its line shape did not change upon a further decrease of the temperature to 213 K. It then became broad until 183 K (Figure 1a). Overall, there is about an ~0.3 ppm upfield shift for the hydride resonance in the variable-temperature ¹H NMR spectra. It is to be noted that no further splitting of the nonet resonance at 3.14 ppm for the hydride in [Ag₈(H){Se₂P(OR)₂}₆]^{+14a} was detected, and only a broad singlet at 5.60 ppm for the hydride was identified in [Ag₈(H){S₂P(OR)₂}₆]^{+14b}. Compound **2_D** exhibits a peak at 9.64 ppm in the ²H NMR spectrum that originates from the entrapped deuteride (Figure 1b). In addition, a band of 17 lines (¹J_{1H–107Ag} = 27 Hz) in the ¹H{¹⁰⁹Ag} spectrum (Figure 1c) is observed, where the intensities of four outermost peaks are too low to be detected. A doublet peak at 1136.1 ppm (¹J_{1H–109Ag} = 32.6 Hz) in the ¹⁰⁹Ag NMR spectrum (Figure 1d), slightly downfield shifted by the comparison with the corresponding resonance of the Ag₈ cube (1056.1 ppm), was observed. The

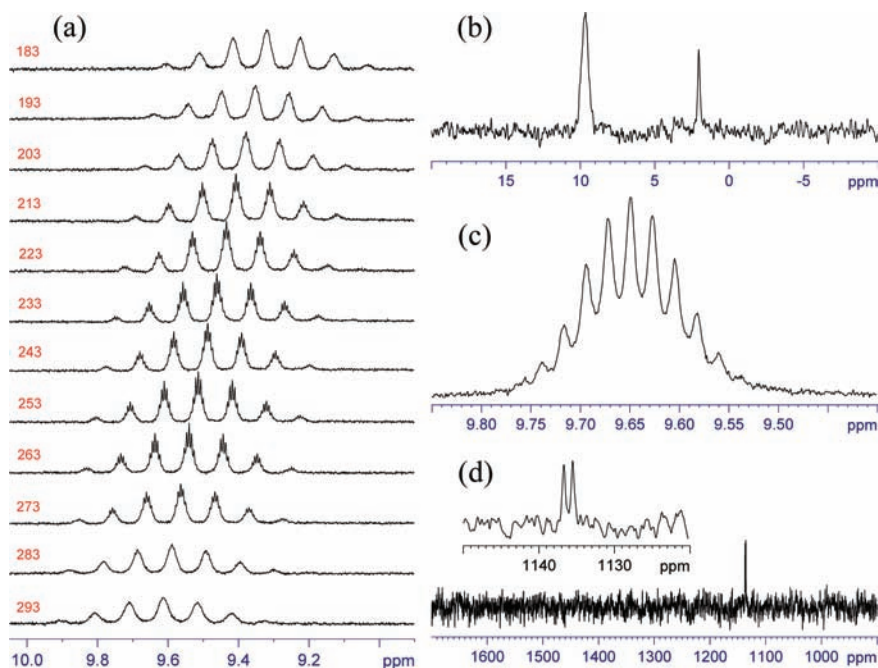


Figure 1. (a) VT (293–183 K) ^1H NMR spectra of 2_{H} . (b) ^2H NMR spectrum of 2_{D} . (c) $^1\text{H}\{^{109}\text{Ag}\}$ NMR spectrum of 2_{H} . (d) ^{109}Ag NMR of 2_{H} with the magnified spectrum shown in the inset.

NMR spectroscopic data strongly suggest that the hydride is coupled to eight, magnetically equivalent silver nuclei on the NMR time scale. Finally, the further splitting into an apparent nonet of nonets attributable to the superposition of the spectra of the different isotopomers was affirmed by the simulated spectrum of an $\text{AX}_8\text{X}'_8$ (X , ^{107}Ag ; X' , ^{109}Ag) spin system. Coupling constants of $J_{\text{1H}-^{107}\text{Ag}}$ (27.0 Hz) and $J_{\text{1H}-^{109}\text{Ag}}$ (31.2 Hz), respectively (Figure 2), were assumed. Presumably, the fast interchange between the capping and vertex silver atoms in 2_{H} causes all eight silver atoms to become equivalent on the NMR time scale (vide infra).^{14a} The ^{13}C NMR spectrum of 2_{H} shows one resonance at 207.0 ppm, which is assigned to the chemical shifts of a CS_2 moiety and shifted slightly compared to the corresponding resonances of the Ag_8 cube (197 ppm).

Three characteristic bands of CN^- stretches, $\text{C}=\text{C}$ stretches, and $\text{C}-\text{S}$ stretches are displayed for all of the complexes (1_{H} , 1_{D} , 2_{H} , and 2_{D}), respectively, in the infrared spectrum (vide supra). In addition, the $\text{M}-\text{S}$ stretching frequency was also identified for these compounds in the range of 193–247 cm^{-1} (see the Experimental Section). The compound 1_{H} exhibits three $\text{Cu}-\text{S}$ stretching bands at 247, 222, and 200 cm^{-1} , which are slightly higher in energy than those observed in the copper compound of $[\text{Cu}(\text{SC}(\text{NHCH}_2)_2)_3]_2(\text{SO}_4)^{15}$ (227 and 214 cm^{-1}) but are similar to those in the Cu_8 cubic cluster (247 and 230 cm^{-1}). Two stretching bands at 225 and 193 cm^{-1} in 2_{H} are assigned to the $\text{Ag}-\text{S}$ stretching frequency, which is not only comparable to the band at 240 cm^{-1} observed in the silver compound, $[\text{AgS}^t\text{Bu}]$,¹⁶ but also close to the $\text{Ag}-\text{S}$ stretching frequency in the Ag_8 cube cluster (220 and 205 cm^{-1}).

Crystallography. 1_{H} . The compound 1_{H} crystallizes in the triclinic $P1$ space group. There are 2 penta-anionic, octanuclear copper clusters, 10 tetrabutylammonium cations, and 1 acetone in the asymmetric unit. The geometry of the copper skeleton is a tetracapped tetrahedron of T_d symmetry, and the eight Cu^{I} ions are further surrounded by six *i*-MNT ligands (Figure 3). In

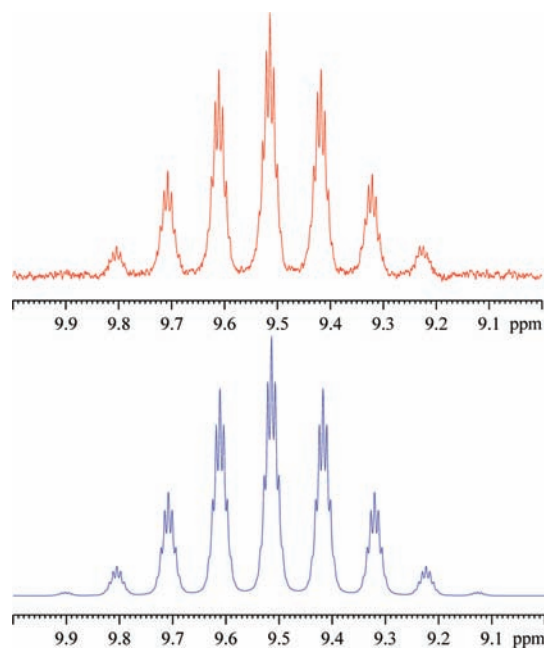


Figure 2. Experimental ^1H NMR spectrum of 2_{H} in *d*-acetone at 253 K (top), and simulated ^1H NMR spectrum of 2_{H} (bottom).

crystallography, the whole copper skeleton is disordered in two orientations (i and ii for cluster 1, iii and iv for cluster 2) with the major component in 75% occupancy. The first group (i) of 1_{H} consists of a tetracapped tetrahedral copper core in which Cu_1 , Cu_5 , Cu_{11} , and Cu_{15} atoms form a tetrahedron (abbr. as Cu_v), and the capping atoms are Cu_3 , Cu_7 , Cu_9 , and Cu_{13} (abbr. as Cu_{cap}). The tetrahedral edge lengths (Cu_v-Cu_v) in the range of 2.892(2)–3.160(2) Å are slightly longer than those of ($\text{Cu}_v-\text{Cu}_{\text{cap}}$) 2.566(2)–2.657(2) Å. The $\text{Cu}_v-\text{Cu}_{\text{cap}}$ distances

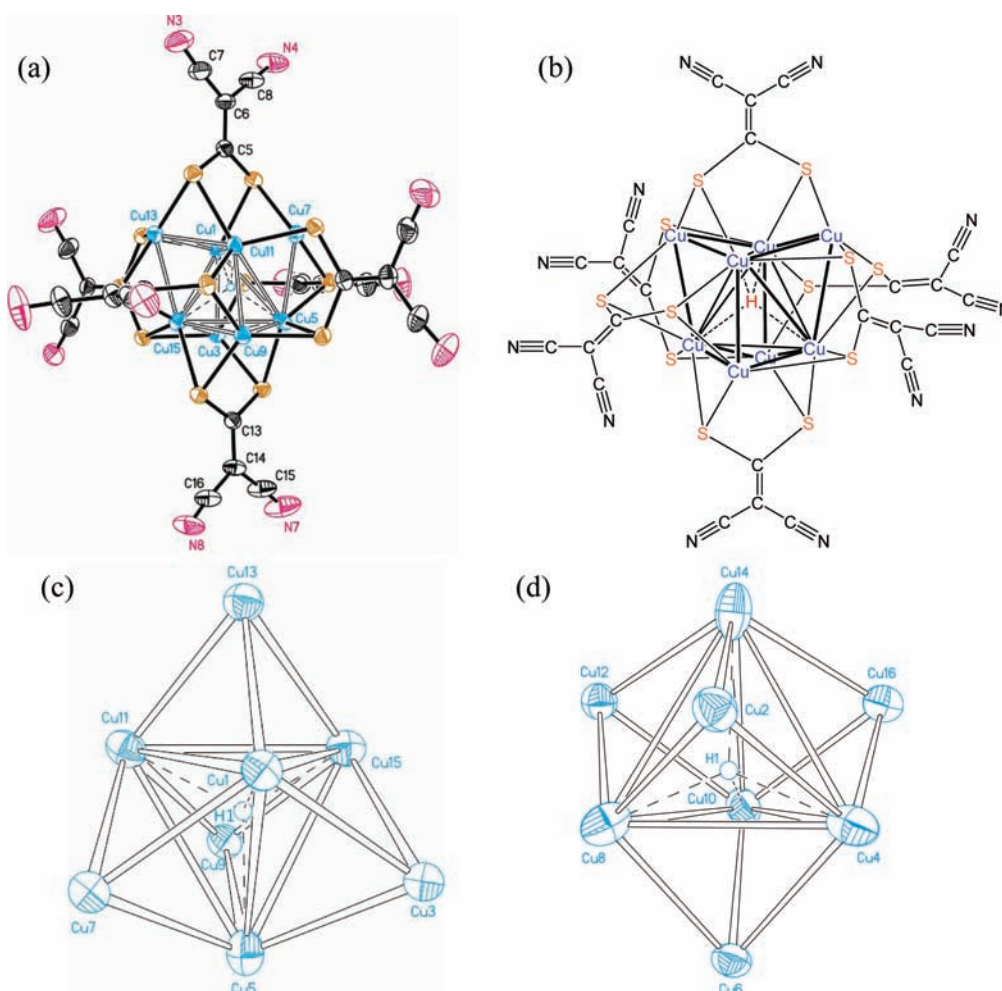


Figure 3. (a) A perspective view of the cluster anion $[\text{Cu}_4(\mu_4\text{-H})(\mu_3\text{-Cu})_4\{\text{S}_2\text{CC}(\text{CN})_2\}_6]^{5-}$ in $\mathbf{1}_\text{H}$ (30% probability ellipsoids). (b) Schematic drawing of $\mathbf{1}_\text{H}$. (c) The Cu_8H core (75% occupancy) in $\mathbf{1}_\text{H}$. (d) The Cu_8H core (25% occupancy) in $\mathbf{1}_\text{H}$.

are much shorter than the sum of van der Waals radii for copper (2.80 Å).¹⁷ In the second group (ii, 25% occupancy), the tetrahedron is composed of Cu4, Cu8, Cu10, and Cu14 (abbr. as Cu_v), and the Cu_v – Cu_v distances lie in the range from 3.077(7) to 3.287(12) Å. However, the distances between capping copper atoms (Cu2, Cu6, Cu12, and Cu16; abbr. as Cu_cap) and vertex copper atoms (Cu_v – Cu_cap) vary from 2.544(6) to 2.673(8) Å. All six, *i*-MNT ligands, each retaining a tetrametallic, tetraconnective bonding mode, are located on the top of Cu_4 butterflies where hinge positions are edges of the tetrahedron and wingtips are four capping atoms. The dihedral angles of the Cu_4 butterflies vary from 162.54(31) to 165.54(30)°. The average intraligand S···S bit distance is 3.070(4), not much different from that of its parent cubane (3.08 Å). Unlike the empty cubic copper cluster $[\text{Cu}_8\{\text{S}_2\text{CC}(\text{CN})_2\}_6]^{4-}$,¹ which displays almost identical Cu–S bond lengths of ~2.251 Å, two kinds of Cu–S distances, namely, Cu_v –S and Cu_cap –S, each averaging 2.372(2) and 2.275(3) Å, respectively, are revealed in $\mathbf{1}_\text{H}$, with the shorter one being associated with the wingtip Cu atoms (Cu_cap). The second copper cluster of $\mathbf{1}_\text{H}$ in the asymmetric unit is isostructural with the first one, and the copper framework is also disordered in two orientations, 75% $\mathbf{1}_\text{H}(\text{iii})$ and 25% $\mathbf{1}_\text{H}(\text{iv})$ occupancy, respectively. The structure of $\mathbf{1}_\text{H}(\text{iii})$ consists of a tetracapped tetrahedral copper core in which Cu19, Cu23, Cu25, and Cu29 (abbr. as Cu_v) atoms

form a tetrahedron, whereas Cu17, Cu21, Cu27, and Cu31 (abbr. as Cu_cap) are the capping atoms. The average edge length of the tetrahedron, (Cu_v – Cu_v) 3.074(2) Å, is slightly larger than Cu_v – Cu_cap [2.548(2) Å]; however, the Cu_v –S distances in $\mathbf{1}_\text{H}(\text{iii})$ (av. 2.379 Å) are longer than Cu_cap –S (av. 2.257 Å). Overall, the compound $\mathbf{1}_\text{H}$ contains 10 quaternary ammonium cations and 2 copper clusters. This establishes the charge of each cluster anion as –5. With the support of ^1H (or ^2H) NMR data, a hydride was placed at the center of the cluster, that is, at the center of the inner Cu_4 tetrahedron, in order to balance the cluster charge. The average Cu– $\mu_4\text{-H}$ distance [1.871(9) Å] is similar to that observed in $[\text{Cu}_8(\text{H})\{\text{S}_2\text{P}(\text{O}^i\text{Pr})_2\}_6]^+$ [1.838(2) Å].⁴ All the relevant metric data are listed in Table 2.

2_H. The compound $\mathbf{2}_\text{H}$ also crystallizes in the triclinic *P1* space group. There are 2 penta-anionic, octanuclear silver clusters, 10 tetrabutylammonium cations, and half of the solvated THF and CH_2Cl_2 molecules, respectively, in the asymmetric unit. In contrast to the presence of two disordered copper frameworks in $\mathbf{1}_\text{H}$, compound $\mathbf{2}_\text{H}$ has one hydride-encapsulated tetracapped tetrahedral silver skeleton where the silver atoms are not disordered. This is evidence that the model used of a disordered metal skeleton for the structural refinement is correct. The tetracapped tetrahedral silver cluster is stabilized within the S_{12} icosahedron by six *i*-MNT ligands (Figure 4). The tetrahedron is formed by the Ag1, Ag2,

Table 2. Selected Bond Lengths (Å) and Angles (deg) for I_H and 2_H with Estimated Standard Deviations Listed in Parentheses

	I_H (i)	I_H (iii)	2_H	2_H (i)
M_V-M_V	1.844(9), 1.874(9), 1.862(9), 1.858(9)	1.787(9), 1.939(9), 1.831(9), 1.973(9)	1.982(10), 2.025(9), 2.062(9), 2.008(10)	1.868(12), 2.033(13), 1.922(12), 2.043(12)
$M_{cap}-H$	2.470(6), 2.516(6), 2.543(7), 2.640(7)	2.462(5), 2.464(4), 2.521(6), 2.628(4)	2.647(11), 2.798(11), 2.891(11), 3.075(10)	2.829(16), 2.847(13), 2.866(14), 2.983(13)
M_V-M_V	2.930(2), 2.8912(19), 3.058(2), 3.022(2), 3.124(2), 3.160(2)	3.032(2), 2.9734(19), 3.093(2), 3.049(2), 3.130(2), 3.166(2)		3.0749(17), 3.1541(19), 3.273(2), 3.1761(18), 3.247(2), 3.337(2),
M_V-M_{cap}	2.625(2), 2.582(2), 2.586(2), 2.580(2), 2.600(2), 2.657(2), 2.610(2), 2.581(3), 2.600(3), 2.566(2), 2.602(2), 2.622(2)	2.5800(16), 2.5748(16), 2.5949(16), 2.6133(17), 2.5990(17), 2.5763(16), 2.5934(17), 2.5824(17), 2.6180(19), 2.570(3), 2.593(2), 2.612(2)	3.0962(12), 3.1501(13), 3.3410(13), 3.2526(13), 3.482(2), 3.416(2)	2.8890(17), 2.8990(18), 2.9083(17), 2.855(2), 2.907(2), 2.913(2), 2.8825(17), 2.9027(17), 2.9275(18), 2.8865(17), 2.8897(17), 2.9038(17)
M_V-S	2.3816(19), 2.3818(19), 2.3909(19), 2.3616(19), 2.356(2), 2.387(2), 2.369(2), 2.371(2), 2.380(2), 2.365(2), 2.3798(19), 2.385(2)	2.3586(16), 2.3608(16), 2.3897(16), 2.3424(16), 2.3586(17), 2.3798(17), 2.3579(17), 2.3836(16), 2.4098(17), 2.3530(19), 2.362(2), 2.380(2)	2.8886(11), 2.8939(11), 2.9236(11), 2.8686(11), 2.8875(11), 2.9076(12), 2.8414(11), 2.9470(12), 2.8900(12), 2.8675(11), 2.8826(11), 2.9270(11)	2.608(3), 2.609(3), 2.647(3), 2.604(3), 2.620(3), 2.678(3), 2.594(3), 2.640(3), 2.680(3), 2.599(3), 2.603(2), 2.620(3)
$M_{cap}-S$	2.248(2), 2.257(2), 2.283(3), 2.254(2), 2.253(2), 2.261(2), 2.265(2), 2.269(2), 2.285(2), 2.250(3), 2.265(3), 2.276(3)	2.2421(17), 2.2613(16), 2.2712(17), 2.2517(17), 2.2581(17), 2.2618(18), 2.2389(16), 2.2581(17), 2.2653(16), 2.2376(17), 2.2645(18), 2.2732(18)	2.515(3), 2.515(3), 2.524(3), 2.514(3), 2.524(2), 2.537(2), 2.525(3), 2.526(3), 2.551(3), 2.521(3), 2.546(3), 2.557(3)	2.507(3), 2.522(3), 2.529(3), 2.497(3), 2.517(3), 2.517(3), 2.494(3), 2.515(3), 2.547(3), 2.485(3), 2.519(3), 2.548(3)
$S \cdots S$ (bite)	3.020(4), 3.025(4), 3.026(5), 3.044(3), 3.074(3), 3.075(5)	3.016(3), 3.025(3), 3.039(3), 3.046(4), 3.048(3), 3.051(4)	3.094(3), 3.098(4), 3.086(3), 3.105(4), 3.099(3), 3.093(3)	3.095(4), 3.094(4), 3.089(3), 3.086(3), 3.092(3), 3.095(4)
dihedral angles of the M_4 butterfly	157.74(10), 158.26(9), 157.64(10), 159.29(10), 157.0(1), 155.13(10),	157.86(8), 161.13(8), 160.31(8), 159.05(7), 160.95(7), 160.16(7)	157.70(10), 155.68(10), 156.46(10), 156.47(10), 156.75(10), 155.86(10)	154.08(10), 155.08(10), 154.78(10), 154.70(10), 155.56(10), 153.81(10)

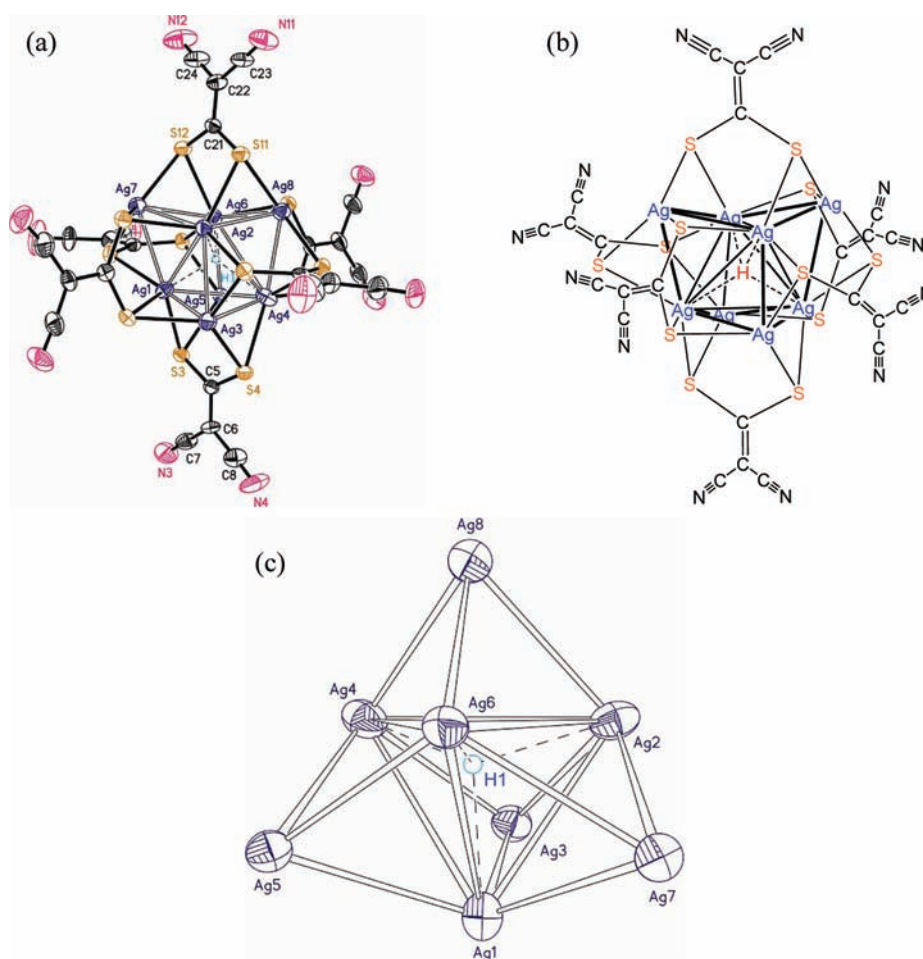


Figure 4. (a) A perspective view of the cluster anion $[Ag_4(\mu_4-H)(\mu_3-Ag)_4\{S_2CC(CN)_2\}_6]^{5-}$ in $2H$ (30% probability ellipsoids). (b) Schematic drawing of $2H$. (c) The Ag_8H core in $2H$.

Ag4, and Ag6 atoms (abbr. as Ag_v), and the capping atoms are Ag3, Ag5, Ag7, and Ag8 (abbr. as Ag_{cap}). The average edge length of the tetrahedron (Ag_v-Ag_v), 3.290(2) Å, which is shorter than twice the van der Waals radius of silver, 1.7 Å,¹⁷ is larger than Ag_v-Ag_{cap} [av. 2.894(2) Å], which is comparable to the covalent radii for silver, 2.90(5) Å.¹⁸ The other silver cluster, $2H(i)$, in which the silver skeleton is disordered in two orientations, has the major component in 75% occupancy. It consists of a tetracapped tetrahedral silver core in which Ag9, Ag10, Ag11, and Ag15 atoms form a tetrahedron (abbr. as Ag_v), with capping atoms Ag12, Ag13, Ag14, and Ag16 (abbr. as Ag_{cap}). The edge of the Ag_4 tetrahedron ranges from 3.075(2) to 3.337(2) Å, and the distances between the capping Ag atom and the vertex of the tetrahedron are in the range of 2.855(2)–2.928(2) Å. All Ag_v-Ag_{cap} distances in $2H$ are slightly shorter than the Ag–Ag distances of the parent cube, 2.957(2)–3.085(2) Å.¹⁹ Six *i*-MNT ligands, each retaining a tetrametallic, tetraconnective bonding mode, are located on the top of Ag_4 butterflies where hinge positions are edges of a tetrahedron and wingtips are two capping Ag atoms. The Ag_v-S distances in $2H$ (av. 2.606(3) Å) are slightly longer than $Ag_{cap}-S$ (av. 2.530(3) Å). Both distances are longer than those observed in the octanuclear cubic silver cluster $[Ag_8(i-MNT)_6]^{4-}$ (av. 2.491 Å).¹⁹ However, the average $S \cdots S$ bite distance in $2H$ (3.096(4) Å) is not only comparable to those in its copper homologue

$[Cu_8(H)\{S_2CC(CN)_2\}_6]^{5-}$ but also identical to those observed in the Ag_8 cube cluster (av. 3.095 Å).¹⁹ Distances between the interstitial hydride and four, directly linked silver atoms are in the range of 1.982(10)–2.062(9) Å. These $Ag-\mu_4-H$ distances are comparable with those identified in $[Ag_8(\mu_4-H)\{E_2P(OR)_2\}_6]^+$ ($E = S, Se$).¹⁴ It is of considerable interest to note that well-characterized, homometallic silver hydrido clusters have been observed to date only in the $Ag_8(H)E_{12}$ ($E = S, Se$) system.

Structural Characteristics. Some comments on the structural characteristics and new findings revealed from the present study are given here:

First, the cluster charge (−5) is strong evidence that the central ion is a hydride in both compounds, corroborating the hydride (deuteride) resonance frequency of the 1H (2H) NMR. The NMR data also rule out one copper atom being Cu(0).

Second, the copper cube does not distort if there is no guest anion in its center. No example of an extremely distorted empty Cu_8 cube surrounded by 1,1-dithio ligands has been reported in the literature.^{2–5} Therefore, the observed distortion of the copper framework from cubic to a tetracapped tetrahedron must be due to the central hydride, which is small and bonds with only four of the eight copper atoms of the cube.

Third, the disordered nature of the copper skeleton, which was previously observed in the hydride-centered M_8 clusters,^{4,5} needs

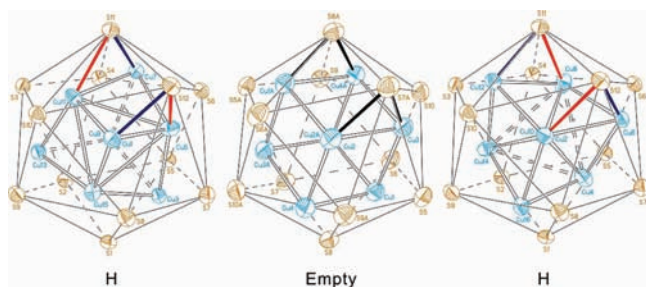


Figure 5. Schematic representations of a tetrahedral contraction of the Cu_8H core in clockwise (left) and counter-clockwise (right) manners from the empty Cu_8 cube (center). All three drawings are viewing down the C_3 of an S_{12} icosahedral cage.

further elaboration. It can be elucidated schematically by examining the two $\text{Cu}_8(\text{H})\text{S}_{12}$ core drawings shown in Figure 5 in which the adjacent $\text{S}\cdots\text{S}$ distance is ~ 3.08 Å. A cube is composed of two interpenetrated tetrahedra. Thus, viewing down the C_3 axis of the cube within the icosahedral sulfur cage in T_h symmetry, the tetrahedral contraction of four of the eight copper atoms occurring in either a clockwise or a counter-clockwise fashion will not only yield two different Cu–S bond lengths [$\text{Cu}_v\text{--S}$, 2.410(2)–2.342(2) (red); $\text{Cu}_{\text{cap}}\text{--S}$, 2.285(2)–2.242(2) Å (blue)] but also produce two interpenetrated tetracapped tetrahedral. The outer one is composed of four Cu_{cap} atoms and the inner one, four Cu_v atoms to which the hydride is connected. Thus, the vertex copper atoms of the tetracapped tetrahedron shown on the left become the capping copper atoms of the other tetracapped tetrahedron depicted on the right, reflections of Cu–S–Cu asymmetric stretches. Though a packing effect cannot be ruled out to produce these structures, the subtle changes in the Cu–S as observed in the stretching vibrations, which are primarily driven by the Cu–H bonding interactions, facilitate the interchange of capping and vertex copper atoms of a tetracapped tetrahedron, thus producing the disordered copper framework. If this hypothesis is correct, the M–S stretching vibrations, where the approximate time scale for IR-Raman data is $\sim 10^{-13}$ s,²⁰ sense the noncubic structure, whereas the NMR in solution, with its longer ($\sim 10^{-9}$ s) time scale,²⁰ shows an average cubic structure. The X-ray results for the solid are modeled best by disorder of the tetracapped tetrahedron of copper atoms.

In conclusion, we have demonstrated that a hydride can be accommodated at the center of an M_8S_{12} icosahedral cluster despite the high overall negative charge (–4) of parent cubic clusters. Considering that the Cu_8S_{12} cluster has been successfully used as the building unit to construct a three-dimensional open framework structure,²¹ it will be of great interest to add hydrides into other Cu_8 cubic cages to study the potential for reversible hydride addition and abstraction. Work in this direction is continuing.

ASSOCIATED CONTENT

S Supporting Information. Crystallographic information for I_H and 2_H (CIF). This material is available free of charge via the Internet at <http://pubs.acs.org>.

AUTHOR INFORMATION

Corresponding Author

*E-mail: chenwei@mail.ndhu.edu.tw (C.W.L.), Fackler@mail.chem.tamu.edu (J.P.F.).

ACKNOWLEDGMENT

Financial support from the National Science Council of Taiwan (NSC 100-2113-M-259-003) is gratefully acknowledged. J.P.F. acknowledges the Welch Foundation of Houston, Texas, Grant A-0960, for support of his work.

REFERENCES

- (1) McCandlish, L. E.; Bissell, E. C.; Coucouvanis, D.; Fackler, J. P.; Knox, K. *J. Am. Chem. Soc.* **1968**, *90*, 7357–7359.
- (2) (a) Hollander, F. J.; Coucouvanis, D. *J. Am. Chem. Soc.* **1974**, *96*, 5646–5648. (b) Hollander, F. J.; Coucouvanis, D. *J. Am. Chem. Soc.* **1977**, *99*, 6268–6280. (c) Dietrich, H.; Storck, W.; Manecke, G. *Makromol. Chem.* **1981**, *182*, 2371–2398. (d) Kanodia, S.; Coucouvanis, D. *Inorg. Chem.* **1982**, *21*, 469–475. (e) Perruchas, S.; Boubekeur, K. *Dalton Trans.* **2004**, 2394–2395. (f) Perruchas, S.; Boubekeur, K.; Auban-Senzier, P. *J. Mater. Chem.* **2004**, *14*, 3509–3515. (g) Baudron, S. A.; Hosseini, M. W.; Kyriatsakos, N. *New J. Chem.* **2006**, *30*, 1083–1086.
- (3) Cardell, D.; Hogarth, G.; Faulkner, S. *Inorg. Chim. Acta* **2006**, *359*, 1321–1324.
- (4) (a) Assavathorn, N.; Davies, R. P.; White, A. J. P. *Polyhedron* **2008**, *27*, 992–998. (b) Liao, P.-K.; Sarkar, B.; Chang, H.-W.; Wang, J.-C.; Liu, C. W. *Inorg. Chem.* **2009**, *48*, 4089–4097.
- (5) Liu, C. W.; Sarkar, B.; Huang, Y.-J.; Liao, P.-K.; Wang, J.-C.; Saillard, J.-Y.; Kahlal, S. *J. Am. Chem. Soc.* **2009**, *131*, 11222–11233.
- (6) (a) Liu, C. W. Ph. D. Dissertation, Texas A&M University, College Station, Texas, 1994. (b) McNeal, C. J.; Liu, C. W.; Song, S.; Huang, Y.; Macfarlane, R. D.; Irwin, M. D.; Fackler, J. P. *Int. J. Mass Spectrom.* **2003**, *222*, 293–501.
- (7) (a) Garland, M. T.; Halet, J.-F.; Saillard, J.-Y. *Inorg. Chem.* **2001**, *40*, 3342. (b) Liu, C. W.; Hung, C.-M.; Santra, B.-K.; Wang, J.-C.; Kao, H.-M.; Lin, Z.-Y. *Inorg. Chem.* **2003**, *42*, 8551–8556.
- (8) Hart, D. W.; Teller, R. G.; Wei, C.-Y.; Bau, R.; Longoni, G.; Campanella, S.; Chini, P.; Koetzle, T. F. *J. Am. Chem. Soc.* **1981**, *103*, 1358–1466.
- (9) Shriver, D. F. *The Manipulation of Air-Sensitive Compounds*, 2nd ed.; Wiley: New York, 1986.
- (10) Sheldrick, G. M. *SADABS*; University of Gottingen: Gottingen, Germany, 1996.
- (11) Sheldrick, G. M. *SHELXL-97: Program for the Refinement of Crystal Structure*; University of Göttingen: Göttingen, Germany, 1997.
- (12) *SHELXL 5.10 (PC Version): Program Library for Structure Solution and Molecular Graphics*; Bruker Analytical: Madison, WI, 1998.
- (13) Liu, C. W.; Staples, R. J.; Fackler, J. P. *Coord. Chem. Rev.* **1998**, *174*, 147–177.
- (14) (a) Liu, C. W.; Chang, H.-W.; Sarkar, B.; Saillard, J.-Y.; Kahlal, S.; Wu, Y.-Y. *Inorg. Chem.* **2010**, *49*, 468–475. (b) Liu, C. W.; Chang, H.-W.; Fang, C.-S.; Sarkar, B.; Wang, J.-C. *Chem. Commun.* **2010**, 46, 4571–4573.
- (15) Bowmaker, G. A.; Pakawatchai, C. P.; Skelton, B. W.; Thavornnyutikarn, P.; Wattananajana, Y.; White, A. H. *Aust. J. Chem.* **1994**, *47*, 15–24.
- (16) Bowmaker, G. A.; Tan, L. C. *Aust. J. Chem.* **1979**, *32*, 1443–1452.
- (17) Bondi, A. J. *Phys. Chem.* **1964**, *68*, 441–445.
- (18) Cordero, B.; Gomez, V.; Platero-Prats, A. E.; Reves, M.; Echeverria, J.; Cremades, E.; Barragan, F.; Alvarez, S. *Dalton Trans.* **2008**, 2832–2838.
- (19) Biker, P. J. M. W.; Verschoor, G. C. J. *Chem. Soc., Chem. Commun.* **1981**, 322–324.
- (20) (a) Muetterties, E. L. *Inorg. Chem.* **1965**, *4*, 769–771. (b) Douglas, B.; McDaniel, D.; Alexander, J. *Concepts and Models of Inorganic Chemistry*, 3rd ed.; Wiley: New York, 1994; p 433.
- (21) (a) Zhang, Z.; Zhang, J.; Wu, T.; Bu, X.; Feng, P. *J. Am. Chem. Soc.* **2008**, *130*, 15238–15239. (b) Behrens, M.; Ordolff, M.-E.; Nather, C.; Bensch, W.; Becker, K.-D.; Guillot-Deudon, C.; Lafond, A.; Cody, J. A. *Inorg. Chem.* **2010**, *49*, 8305–8309.